Journal of Mathematics Research

http://ccsenet.org/jmr

Vol. 2, No. 1

February 2010

A Model to Study Effect of Rapid Buffers and Na^+ on Ca^{2+} Oscillations in Neuron Cell

Vikas Tewari (Corresponding author)

Department of Mathematics, Maulana Azad National Institute of Technology

Bhopal 462 051, (M.P.), India

Tel: 91-998-123-2944 E-mail: vikastewari1@rediffmail.com

Shivendra Tewari

Department of Mathematics, Maulana Azad National Institute of Technology

Bhopal 462 051, (M.P.), India

Tel: 91-982-623-6524 E-mail: shivendra.tewari@hotmail.com

K. R. Pardasani

Department of Mathematics, Maulana Azad National Institute of Technology

Bhopal 462 051, (M.P.), India

Tel: 91-942-535-8308 E-mail: kamalrajp@rediffmail.com

Abstract

Ca^{2+} plays a vital role in muscle mechanics, cardiac electrophysiology, secretion, hair cells, and adaptation in photoreceptors. It is a vital second messenger used in signal transduction. Calcium controls cell movement, cell differentiation, ciliary beating. Many cells exhibit oscillations in intracellular [Ca^{2+}] in response to agonist such as hormones and neurotransmitters. Many cells use oscillations in calcium concentration to transmit messages (Sneyd J. *et al*, 2006, p. 151-163). In this paper, an attempt has been made to develop a model to study calcium oscillations in neuron cells. This model incorporates the effect of variable Na^+ influx, sodium-calcium exchange (NCX) protein, Sarcolemmal Calcium ATPase (SL) pump, Sarco-Endoplasmic Reticulum CaATPase (SERCA) pump, sodium and calcium channels, and IP_3R channel. The proposed mathematical model leads to a system of partial differential equations which has been solved numerically using Forward Time Centered Space (FTCS) approach. The numerical results have been used to study the relationships among different types of parameters such as buffer concentration, disassociation rate, calcium permeability, etc.

Keywords: Signal transduction, Calcium oscillations, Na^+ influx, NCX protein, SL pump, SERCA pump, IP_3R channel, FTCS approach

1. Introduction

Calcium oscillations are known to play a key role in a number of mechanisms like the secretion in the pituitary and parotid glands, the contraction of smooth muscle, and cardiac inotrophy and induction of arrhythmias (Jafri M.S. *et al*, 1992, p. 235-246). These oscillations are supposed to contain frequency encoded signals that help in using Calcium as a second messenger while avoiding its high intracellular concentrations (Keener J. *et al*, 1998, p. 53-56). A number of investigators have reported the oscillatory behaviour of calcium due to intracellular concentration of inositol 1, 4, 5-trisphosphate (IP_3). In the process of signal transduction, intracellular calcium acts like a switch and decides whether a particular signal needs to be further propagated or not.There are mainly two types of receptors, Rynodine Receptors (RyRs) or Inositol Triphosphate Receptors (IP_3Rs) that are located at the membrane of endoplasmic reticulum (in neurons) or sarcoplasmic reticulum (in myocytes) which cause an efflux of Ca^{2+} in the cytosol. The release of Ca^{2+} through IP_3Rs is as a result of some agonist or neurotransmitter binding to its receptor which can cause via G protein link to phospholipase C (PLC), the cleavage of phosphotidylinositol (4,5)-bisphosphate (PIP_2) to inositol triphosphate (IP_3) and diacylglycerol (DAG). This released IP_3 is free to diffuse through the cytosol and binds with IP_3R leading to the subsequent opening of these

receptors and release of Ca^{2+} from the intracellular stores. Calcium oscillation can be classified into mainly two types: 1) that is induced by changing membrane potential as in the case of an action potential and the associated periodic entry of Ca^{2+} through voltage-gated Ca^{2+} channels,2) that occur in the presence of voltage clamp. The latter part can be further categorized based on the fact that the oscillatory Ca^{2+} flux is from RyRs or IP_3Rs. The period of IP_3-dependent oscillations ranges from a few seconds to a few minutes. There is a great deal of evidence that in many cell types, these oscillations occur at constant $[IP_3]$ and are therefore not driven by oscillations in $[IP_3]$. It is also observed that as $[IP_3]$ increases, the steady state $[Ca^{2+}]$ increases, the oscillation frequency increases, and the amplitude of the oscillations remains approximately constant. Calcium oscillations usually occur only when $[IP_3]$ is greater than some critical value and disappear again when $[IP_3]$ gets too large. Thus, there is an intermediate range of IP_3 concentrations that generate Ca^{2+} oscillations (Keener J. *et al*, 1998, p. 53-56).In this paper, we have also studied oscillations induced in calcium due to change in IP_3 concentration. Here a mathematical model is proposed which incorporates nearly all important and necessary biophysical parameters like buffers, L-type calcium channel, calcium pump, sodium calcium exchanger (NCX), and calcium leak. Further, we assume that buffers exhibit rapid buffering.

Another factor which might have significant effect on calcium oscillation and which has not been given much importance is the sodium ion concentration. We have incorporated it through the NCX protein. We have considered an exchange ratio of 4:1 (Fujioka Y., 2000, p.611-623) with respect to sodium and calcium ions respectively. To make the model more realistic we have included the ER. The proposed mathematical model leads to a system of partial differential equations. We have used finite difference approach for the simulation of the proposed model for which a program has been developed in MATLAB and run on a Pentium IV Dual Core 1.00 GB RAM, 1.73GHz processor to obtain the numerical result. The time taken per simulation is 240 seconds for time, t = 30 seconds.

2. Mathematical Model

Our mathematical model assumes the following reaction-diffusion kinetics (Wagner J. *et al*, 1994, p.447-456) (Smith G.D., 1996, p.3064-3072),

$$[Ca^{2+}] + [B_m] \underset{k^-}{\overset{k^+}{\rightleftarrows}} [CaB_m] \tag{1}$$

where, $[B_m]$ and $[CaB_m]$ are free and bound buffers respectively. Using Ficks law of diffusion and law of mass action and assuming rapid buffering approximation, we have the following partial differential equation (Smith G.D., 1996, p.3064-3072),

$$\frac{\partial [Ca^{2+}]}{\partial t} = \beta \left(D_{Ca} + \gamma_m D_{CaBm}\right) \nabla^2 \left[Ca^{2+}\right] - \frac{2\beta\gamma_m D_{CaBm}}{K_m + [Ca^{2+}]} \nabla \left[Ca^{2+}\right] . \nabla \left[Ca^{2+}\right] \tag{2}$$

$$\begin{aligned} &\textit{where,} \\ &\beta = (1 + \gamma_s + \gamma_m)^{-1} \textit{ and} \\ &\gamma_m = \frac{K_m [B_m]_T}{(K_m + [Ca^{2+}])^2} \end{aligned}$$

D_{Ca}, and D_{CaB_m} are the diffusion coefficients of free calcium, and calcium bound buffer respectively, and K_m is disassociation rate constant. For stationary buffers, $D_{CaBm} = 0$.

Our proposed mathematical model also contains the following parameters, to study the effect of rapid buffer, Na^+ ions and ER over Ca^{2+} oscillations,

2.1 Ion channels

The Ca^{2+} and Na^+ channels have been modeled using the Goldman-Hodgkin-Katz (GHK) current equation (Keener J. *et al*, 1998, p. 53-56):

$$I_s = P_s z_s^2 \frac{F^2 V_m}{RT} \frac{[S]_i - [S]_o \exp\left(-\frac{z_s F V_m}{RT}\right)}{\left(1 - \exp\left(-\frac{z_s F V_m}{RT}\right)\right)} \tag{3}$$

where $[S]_i$,$[S]_o$, are the intracellular and extracellular ion concentration (Molar),respectively .P_S is the permeability (m/s) of S ion, z_s is valence of S ion. F is Faradays constant (C/moles).V_m is membrane potential (Volts). R is Real gas constant (J/K moles) and T is Absolute temperature (Kelvin). Equation (3) is converted into molar/second by using the following equation

$$\sigma_s = \frac{-I_s}{z_s F V_{cyt}} \tag{4}$$

The negative sign in equation (4) is taken because by convention inward current is taken to be negative. The GHK equation is derived from the constant field approximation which assumes that the electric field in the membrane is constant, and thus decoupled from the effects of charges moving through the membrane.

2.2 Na^+ / Ca^{2+} Exchange (NCX) Protein

The NCX protein is essential for excitation-contraction coupling in cardiac myocytes (Fujioka Y., 2000, p.611-623). It helps in the extrusion of cytosolic calcium in neurons and hence regulates neurotransmitter release, (Blaustein M.P., 1999, p. 763-854). The pump is assumed to be electrogenic in nature as one calcium leaves the cytosol for intake of four sodium ions. In our model we have taken an exchange ratio of 4:1 with respect to sodium and calcium ions respectively (Fujioka Y., 2000, p.611-623). The amount of energy required to extrude an ion against its concentration gradient is given by:

$$\Delta_s = z_s F V_m + RT \log\left(\frac{S_i}{S_o}\right) \tag{5}$$

So using $\triangle Ca^{2+} = 4\triangle Na^+$, we have,

$$\sigma_{NCX} = Ca_o \left(\frac{Na_i}{Na_o}\right)^4 \exp\left(\frac{2FVm}{RT}\right) \tag{6}$$

$$\overline{\sigma}_{NCX} = Na_o \left(\frac{Ca_i}{Ca_o}\right)^{1/4} \exp\left(-\frac{FVm}{2RT}\right) \tag{7}$$

2.3 Sarcolemmal Calcium ATPase pump (SL CaATPase pump)

It is a P-type ATPase which is also known as Plasma Membrane Calcium ATPase pump (PMCA). Energy obtained from ATP is used to extrude calcium ions out of the cytosol. The kinetics of the pump follows MichaelisMenten kinetics (Nelson D.L., 2005) (Blackwell K.T., 2005, p.1-27). So the net efflux of calcium ions out of the cytosol is given by:

$$\sigma_{SLPump} = \frac{V_{SLPump}}{1 + \left(\frac{K_{SLPump}}{Ca_i}\right)^H} \tag{8}$$

where, V_{SLpump} is the maximum pump capacity, K_{SLpump} is half of the maximum pump capacity at steady state and H is the Hills coefficient.

2.4 Sarco Endoplasmic Reticulum CaATPase (SERCA) pump

The SERCA pump uses the chemical energy produced from the conversion of adenosine triphosphate (ATP) into adenosine diphosphate (ADP) to transport calcium ions across the membrane from the cytosol to the ER, against its concentration gradient, (Sneyd J. *et al*, 2006, p. 151-163). It binds calcium on the cytosolic side and releases it on the ER side. The SERCA pump has been modelled by a simple Hills equation as follows:

$$\sigma_{SERCApump} = \frac{v_{SERCA}}{1 + \left(\frac{k_{SERCA}}{Ca_i}\right)^H} \tag{9}$$

where, v_{SERCA} is the maximal pump rate, k_{SERCA} is half of the maximum pump capacity at steady state and H is the Hills coefficient.

2.5 Endoplasmic Reticulum leak and IP_3R Flux

There is a certain amount of leak from the ER to the cytosol along the concentration gradient and an IP_3 flux given by the following term (Jafri S. *et al*, 1995, p.2139-2153):

$$c_1(leakcons + ipflux((X_{110})_i^j)^3)((u_{er})_i^j - u_i^j) \tag{10}$$

Where, c_1 is the ratio of volume of ER to cytosol, leakcons is the calcium leak rate constant, ipflux is the maximum IP_3 receptor flux, X_{110} fraction of open channels; u_{er} and u are the calcium concentrations in the ER and cytosol respectively.

Variation of channel states, that is, whether closed or opened is given as follows

$$\frac{dX_{100}}{dt} = -a_2[Ca^{2+}]X_{100} - a_5[Ca^{2+}]X_{100} + b_5X_{110} \tag{11}$$

$$\frac{dX_{110}}{dt} = -a_2[Ca^{2+}]X_{110} + b_2c_2[IP_3] + a_5[Ca^{2+}]X_{100} - b_5X_{110} \tag{12}$$

Where, X_{100} and X_{110} represent the fraction of closed channels and open channels respectively.a_2 is inhibitory receptor binding constant,a_5 is activation receptor binding constant, b_2 is inhibitory receptor disassociation constant, and b_5 is activation receptor disassociation constant.

2.6 ER Calcium Concentration

Calcium in the ER is assumed to be under rapid buffering approximation (Jafri S. *et al*, 1995, p.2139-2153), and is as given below,

$$\frac{\partial[Ca^{2+}]_{ER}}{\partial t} = \left(\frac{1}{c_1}\right)\beta_{ER}\begin{pmatrix} \left(\left(D_{Ca}^{ER} + \gamma_m^{ER} D_{CaBm}^{ER}\right)\nabla^2[Ca^{2+}]_{ER} - \frac{2\gamma_m^{ER} D_{CaBm}^{ER}}{K_m^{ER}+[Ca^{2+}]_{ER}}\nabla[Ca^{2+}]_{ER}.\nabla[Ca^{2+}]_{ER}\right).c_1 \\ -c_1\left(v_2 + v_1 X_{110}^3\right)\left([Ca^{2+}]_{ER} - [Ca^{2+}]\right) + \frac{v_3[Ca^{2+}]^2}{k_3^2+[Ca^{2+}]^2} \end{pmatrix} \tag{13}$$

$$where,\ \ \beta_{ER} = \left(1 + \frac{K_s^{ER}[B_s]_{ER}}{\left(K_s^{ER} + [Ca^{2+}]_{ER}\right)^2} + \frac{K_m^{ER}[B_m]_{ER}}{\left(K_m^{ER} + [Ca^{2+}]_{ER}\right)^2}\right)^{-1} \ and$$

$$\gamma_m^{ER} = \frac{K_m^{ER}[B_m]_{ER}}{\left(K_m^{ER} + [Ca^{2+}]_{ER}\right)^2}$$

2.7 $[IP_3]$ *Variation*

The IP_3 concentration varies with time according to the equation given below, (Keizer J. *et al*, 1992, p. 649-660)

$$\frac{d[IP_3]}{dt} = v_3 f(t) + \frac{v_6[Ca^{2+}]_i}{k_6 + [Ca^{2+}]_i} - v_7[IP_3] \tag{14}$$

where, f(t)=0 or 1 (defines pulses of IP_3), v_3 is external IP_3 input rate, v_6 is maximum calcium dependent IP_3 input rate, v_7 is IP_3 decay rate constant and k_6 is activation constant, calcium dependent IP_3 input. The first term in above equation denotes IP_3 pulse, second term denotes calcium induced IP_3 production and last term denotes IP_3 degradation.

Combining equations (1-14) we get the proposed mathematical model as given below,

$$\frac{\partial[Ca^{2+}]}{\partial t} = \beta\left(D_{Ca} + \gamma_m D_{CaBm}\right)\nabla^2\left[Ca^{2+}\right] - \frac{2\beta\gamma_m D_{CaBm}}{Km + \left[Ca^{2+}\right]}\nabla\left[Ca^{2+}\right].\nabla\left[Ca^{2+}\right]$$
$$\sigma_{NCX} - \sigma_{SLPump} - \sigma_{SERCA} + \sigma_{ERleak} \tag{15}$$

$$\frac{\partial[Na^+]}{\partial t} = \beta_{sod}\left(-\sigma_{Na} + \sigma_{NCX} - \sigma_{leak}\right) \tag{16}$$

Along with the initial-boundary conditions,

A. Initial condition:

$$[Ca^{2+}]_{t=0} = 0.1\mu M and [Na^+]_{t=0} = 12mM \tag{17}$$

B. Boundary conditions:

$$\lim_{r\to 0}\left(-2\pi r^2\beta\left(D_{Ca} + \gamma_m D_{CaBm}\right)\frac{d[Ca^{2+}]}{dr}\right) = \beta\sigma_{Ca} \tag{18}$$

$$\lim_{r\to\infty}[Ca^{2+}] = 0.1\mu M \tag{19}$$

Our problem is to solve equation (15) and (16) coupled with equation (17-19). For our convenience we are writing 'u' in lieu of $[Ca^{2+}]$ and 'v' in lieu of $[Na^+]$. Applying finite difference method (Forward Time Centered Space) on equation (15 16), we get

$$\frac{u_i^{j+1} - u_i^j}{k} = \beta_i^j\begin{pmatrix} \left(D_{eff}\right)_i^j\ \frac{(u_{i+1}^j - 2u_i^j + u_{i-1}^j)}{(h^2)}\ ) + \frac{(u_{i+1}^j - u_{i-1}^j)}{h}(\frac{D_{eff_i}^j}{r_i} - \frac{((\gamma_m\ _i^j D_m)(u_{i+1}^j - u_{i-1}^j))}{(2h(K_m + u_i^j))}\ ) \\ +c_1(leakcons + ipflux((X_{110})_i^j)^3)((u_{er})_i^j - u_i^j) - \frac{sprate*(u_i^j)^2}{((u_i^j)^2 + spdissrat^2)} \\ -\frac{1}{(1+\ e^{(v_i^j - 130)/14}\ )}u_{out}\left(\frac{v_i^j}{v_{out}}\right)^4 e^{2\varepsilon} - \frac{V_{SLpump}}{1+\left(\frac{K_{SLpump}}{u_i^j}\right)^{1.6}} \end{pmatrix}$$

And

$$\frac{v_i^{j+1}-v_i^j}{k}=\beta_{sod_i^j}\left(\frac{1}{\left(1+\ e^{(v_i^j-130)/14)}\right)}v_{out}\left(\frac{u_i^j}{u_{out}}\right)^{(1/4)}e^{(-\varepsilon/2)}+\frac{k_{Cain}}{(k_{Cain}+u_i^j)}\frac{((3*10^5)P_{Na}\ \varepsilon)}{(1-e^{\varepsilon})}(v_i^j e^{\varepsilon}-v_{out})-P_L(v_{out}-v_i^j)\right) \tag{20}$$

where, $\varepsilon = FV_m/RT$ is a dimensionless quantity, 'h' represents spatial step and 'k' represents time step, 'i' and 'j' represents the index of space and time respectively. Since, the above expression is not valid at the mouth of the channel; therefore the approximation at the mouth of the channel is given by

$$u_1^{j+1}=k.\beta_1^j\left(\begin{array}{l}\left(\left(D_{eff}\right)_1^j\ \frac{(2u_2^j-2u_1^j)}{(h^2)}\ \right)+c_1(leakcons+ipflux((X_{110})_1^j)^3)((u_{er})_1^j-u_1^j)\\ -\frac{sprate*(u_1^j)^2}{((u_1^j)^2+spdissrat^2)}\ -\frac{1}{(1+\ e^{(v_1^j-130)/14}\ )}u_{out}\left(\frac{v_1^j}{v_{out}}\right)^4 e^{2\varepsilon}\\ -\frac{V_{SLpump}}{1+\left(\frac{K_{SLpump}}{u_1^j}\right)^{1.6}}+sigma\end{array}\right)+u_1^j \tag{21}$$

And

$$v_1^{j+1}=k.\beta_{sod_1^j}\left(\frac{1}{\left(1+e^{(v_1^j-130)/14)}\right)}v_{out}\left(\frac{u_1^j}{u_{out}}\right)^{(1/4)}e^{(-\varepsilon/2)}+\frac{k_{Cain}}{(k_{Cain}+u_1^j)}\frac{((3*10^5)\ P_{Na}\varepsilon)}{(1-e^{\varepsilon})}(v_1^j e^{\varepsilon}-v_{out})-P_L(v_{out}-v_1^j)\right)+v_1^j \tag{22}$$

3. Result and Discussion

In this section the results and discussion of the obtained numerical solution is given. The values of all the biophysical parameters used are as given in table 1. Figures (1-6) are the plots obtained for $[IP_3] = 0.6\mu$M whereas figures (7-12) are obtained for variable IP_3 concentration.

Mobile Buffers (Simulation Time =48s)

Figure 1 shows the oscillations in calcium concentration against time with variable mobile buffer concentration for a constant $[IP_3]$ concentration of 0.6μM. This figure shows that it is not necessary to have oscillations in $[IP_3]$ to observe oscillations in calcium concentration, (Keizer J. *et al*, 1992, p. 649-660). As the buffer concentration increases the free calcium concentration decreases but in the time interval t= [8-15]s and t= [27-30]s it is vice-versa. The reason for this is that as the calcium concentration increases the NCX protein activates which causes larger extrusion of calcium ions from the cytosol. Hence the calcium concentration inside the cytosol decreases.

Figure 2 shows the variation with time and buffer disassociation rate for two mobile endogenous buffers, calmodulin (K_m=2μM) and (K_m=3μM). As the disassociation rate increases more calcium ions become free and so the calcium concentration increases. However, in the time duration [7-15]s and [25-30]s it is vice-versa, i.e., lower disassociation rate has higher calcium concentration. This is because as the calcium ions increases the NCX protein activates which extrudes 1 calcium ion for four sodium ions entering the cytosol. Also the frequency has increased on increasing the buffer disassociation rate. This is due to the faster kinetics involved with higher disassociation rate. Also there is latency in the oscillation, that is, delay in time required to attain maximum value. When the disassociation rate is increased the calcium achieves the peak value faster.

Stationary buffers (Simulation Time =48s)

Figure 3 shows that as the stationary buffer concentration increases the calcium concentration decreases as more number of ions get bound to the buffer. However, in the intervals t= [7-15]s and [26-30]s the trend reverses. This is due to the fact that initially only the Sarcolemmal pump is working but as the calcium concentration increases the NCX protein gets activated which extrudes larger amount of calcium ions from the cytosol and hence the concentration decreases. The stationary buffers are immobile and hence they affect only the temporal variation of calcium and do not affect the spatial profile. The Calcium achieves the peak value faster when the buffer concentration is lower. This explains the latency observed.

Figure 4 shows variations in calcium concentration with time and buffer disassociation rate. Initially calcium concentration increases with increase in disassociation rate. This is so because with increases in disassociation rate more calcium ions

become free. However in the time intervals [8-15]s and [26-30]s calcium decreases with increase in disassociation rate. This is because as the calcium ions reach higher concentrations the NCX protein gets activated which extrudes more calcium ions and hence the calcium ion concentration inside the cytosol decreases. As the buffer disassociation rate increases the frequency of oscillation also increases. This is because higher disassociation rate implies faster Calcium kinetics, that is, the binding and disassociation increases. We also observe latency in the oscillations. As the disassociation rate is increased the peak value is achieved faster.

Figure 5 shows the variations of calcium concentration with time and the leak rate constant of calcium from the ER into the cytosol are as shown in the above figure. As the calcium leak from the ER into the cytosol is increased the amount of free calcium in the cytosol increases. However, in intervals [5-12]s and [24-30]s the opposite is observed because with increase in calcium ions the NCX protein extrudes larger amount of calcium ions and hence the net calcium ion concentration in the cytosol decreases.

Figure 6 shows the sodium concentration variation with time. For the sodium concentration we have incorporated (1) sigmoidal deactivation of the NCX protein (2) calcium dependent inactivation of the L-type sodium channel and (3) a leak term which balances the sodium entering the cytosol via sodium channel and NCX protein. The sodium decreases up to 4s and thereafter increases. It decreases first due to deactivation of the NCX protein and calcium dependent inactivation of the sodium channel. After that it increases as the NCX protein is no longer deactivated and the sodium channel is also no longer inactivated.

Variable IP_3

Figure 7 shows a comparison of calcium concentration and IP_3 concentration on time scale. It is observed that the peaks of calcium and IP_3 occur at about the same time. This is because IP_3 oscillations are believed to induce calcium oscillations. By incorporating variable IP_3 it is observed that the frequency of calcium oscillation increases. Since earlier we observed only two peaks in 30 s time interval but now we observe 3 peaks. This has also been proved by Kusters *et al*, (Kusters *et al*, 2005, p. 3741-3756).Calcium is released from the ER when the IP_3 binds to the IP_3R and is refilled back into the ER by the SERCA pump. This increases and decreases the calcium in cytosol more rapidly when we consider a varying IP_3 which is dependent on the fraction of open channels. Also the calcium maximum concentration increases from 0.37 μM to 0.7 μM. This is because of increased released of calcium from the ER. In the earlier case we had taken the IP_3 value to be 0.6 μM whereas the maximum IP_3 value here is 1.15 μM. IP_3 is regulated by the fraction of open channels in the ER which regulates the amount of calcium released from the ER.

Figure 8 compares cytoplasmic and ER calcium concentration on time scale. Both show oscillations with respect to time. Calcium concentration is high in the ER compared to the cytoplasm. There is a leak of calcium from the ER to the cytoplasm and calcium uptake by ER through the SERCA pump. It is thus observed that when the calcium concentration in the ER is minimum it has a maximum in the cytoplasm. This has also been proved by Kusters *et al*, (Kusters *et al*, 2005, p. 3741-3756).It is also observed that the calcium concentration in the ER is continuously decreasing. This is so because the calcium extrusion from the cytosol via the NCX protein and Sarcolemmal pump is large and hence the amount of calcium being refilled into the ER by the SERCA pump is decreasing.

Figure 9(a) depicts variation of cytosolic calcium variation with ER buffer concentration and time. The effects of changing buffer concentration are negligible near the source due to rapid buffering. As we move away from the source the effect of other parameters becomes visible. So the effects are more visible at the second peak compared to the first peak. It is observed that as the ER buffer concentration increases the cytosolic calcium increases. This is because as ER buffer concentration increases more calcium inside the ER gets bound to the buffers so concentration gradient decreases and hence lesser calcium ions leak from the ER to cytosol. The pumping by the SERCA pump depends on the cytosolic calcium concentration which pumps lesser amount of calcium from the cytosol and hence the cytosolic calcium concentration increases. Also ER buffer concentration has little effect on cytoplasmic calcium oscillations. This is in agreement with the findings of Kusters *et al* (Kusters *et al*, 2005, p. 3741-3756).

Figure 9(b) depicts variation of cytosolic calcium variation with cytosolic buffer concentration and time. The effects of changing buffer concentration are less near the source due to rapid buffering. So the effects are more visible at the second peak compared to the first peak. It is observed that as the cytosolic buffer concentration increases the cytosolic calcium decreases. This is because as buffer concentration increases more calcium in the cytosol gets bound to the buffers. Hence the cytosolic calcium concentration decreases.

Figure 10(a) depicts variation of ER calcium concentration with ER buffer concentration and time. The effects of changing buffer concentration are more evident at the second peak compared to the first peak due to rapid buffering in the ER. It is observed that as the ER buffer concentration increases the ER calcium increases. This is because as ER buffer concentration increases more calcium inside the ER gets bound to the buffers so there is lesser concentration gradient so lesser calcium ions leak from the ER. Hence the ER calcium concentration increases.

Figure 10(b) depicts variation of ER calcium concentration with cytoplasmic buffer concentration and time. As the cytoplasmic buffer increases more calcium ions inside the cytosol get bound. The refilling by SERCA pump is proportional

to the cytosolic calcium so lesser cytosolic calcium implies that there is lesser refilling of the ER and hence the ER calcium concentration decreases. Also as calcium concentration in the cytoplasm decreasing there is more concentration gradient and hence more calcium leaks from the ER and hence the ER calcium concentration decreases.

Figure 11(a) depicts variation of cytosolic calcium variation with ER buffer disassociation rate and time. The effects of changing buffer disassociation rate are negligible at first spike due to rapid buffering. As we move away from the source the effect of disassociation rate becomes more evident. It is observed that as the ER buffer disassociation rate increases the cytosolic calcium increases. This is because as ER buffer disassociation rate increases more calcium inside the ER becomes free so there is a larger leak of calcium ions from the ER into the cytosol. Thus calcium ion concentration inside the cytosol increases. ER buffer disassociation rate has negligible effect on cytosolic calcium oscillations as also shown by Kusters *et al* (Kusters *et al*, 2005, p. 3741-3756).

Figure 11(b) depicts variation of cytosolic calcium variation with cytoplasmic buffer disassociation rate and time. The results are evident, that is, as the disassociation rate increases the calcium concentration in the cytosol also increases.

Figure 12(a) depicts variation of ER calcium concentration with ER buffer disassociation rate and time. The effects of changing buffer disassociation rate are more evident at second spike due to rapid buffering. It is observed that as the ER buffer disassociation rate increases the ER calcium increases, this is in agreement with the physiological facts. As ER buffer disassociation rate increases more calcium inside the ER gets free. This is because disassociation rate is the ratio of disassociation to association rate, so larger disassociation rate implies that disassociation is greater than association so more calcium ions are released from the buffer.

Figure 12(b) depicts variation of ER calcium concentration with cytosolic buffer disassociation rate and time. As the cytosolic buffer disassociation rate increases the calcium concentration inside the cytosol increases and hence a greater amount of refilling of calcium into the ER by the SERCA pump. Hence the calcium concentration inside the ER increases. Also the concentration gradient across the ER decreases and hence there is less amount of calcium leaking from the ER into the cytosol so the ER calcium concentration increases.

4. Conclusion

Here we have studied the effects of sodium ions on calcium oscillations which have not been given much importance till date. We have used an exchange ratio of 4:1 with respect to sodium and calcium ions. We have tried to make the model more realistic by incorporating the different parameters as mentioned above. Some of the results obtained above are in agreement with the work done by previous researchers. The new results obtained are also in agreement with the physiological facts. The numerical solutions obtained above can be used to study the relationships among different types of parameters in the normal and abnormal conditions which can be useful to biomedical scientists for developing new protocols for the diagnosis and treatment of various neurological diseases.

Acknowledgment

The authors are highly grateful to Department of Biotechnology, New Delhi, India and Madhya Pradesh Council for Science and Technology,Bhopal, India for providing support in the form of Bioinformatics Infrastructure Facility for carrying out this work.

References

Blackwell K.T. (2005). *Modeling Calcium Concentration and Biochemical Reactions*, Brains Minds and Media, pg. 1-27, (Chapter 1).

Blaustein M. P.& Lederer W. J. (1999). Sodium / Calcium Exchange: Its Physiological Implications. *Physiol. Rev.* Vol.79, pg.763-854.

Fain G. L. (1999). *Molecular and Cellular Physiology of Neurons*, Harvard University Press, (Chapters 1, 3, 4).

Fujioka Y., Hiroe K.& Matsuoka S. (2000). Regulation kinetics of Na^{+}-Ca^{2+} Exchange Current in Guinea-Pig Ventricular Myocytes. *Journal of Physiology*, Vol. 529, pg. 611-623.

Jafri S.& Keizer J. (1995). On the Roles of Calcium Diffusion, Calcium buffers, and the Endoplasmic Reticulum in IP_3-induced Calcium Waves. *Biophysical Journal*, Vol. 69, pg.2139-2153.

Jafri M. S., Vajda S. P., Pasik S. & Gillo B. (1992). A Membrane Model for Cytosolic Calcium Oscillations: A Study using Xenopus oocytes. *Biophysical Journal*, Vol. 63, pg, 235-246.

Keener J. & Sneyd J. (1998). *Mathematical Physiology*, (Vol. 8), Springer, pg. 53-56, (Chapter 2).

Keizer J. & Young G.W.D. (1992). Two Roles for Calcium in Agonist-Stimulated Calcium Oscillations. *Biophysical Journal*, Vol. 61, pg. 649-660.

Kusters *et al*. (2005). Stabilizing Role of Calcium Store-Dependent Plasma Membrane Calcium Channels in Action-Potential Firing and Intracellular Calcium Oscillations. *Biophysical Journal*, Vol. 89, pg. 3741-3756.

Nelson D. L. & Cox M. M. (2005). *Lehninger Principles of Biochemistry*, (4th ed.),University of Wisconsin-Madison, (Chapter 6).

Shannon T. R., Wang F., Puglisi F., Weber C. & Bers D. M. (2004). A Mathematical Treatment of Integrated Ca^{2+} Dynamics within the Ventricular Myocyte. *Biophysical Journal*, Vol. 87, pg. 3351 – 3371.

Smith G.D. (1996). Analytical Steady-State Solution to the Rapid Buffering Approximation near an Open Ca^{2+} Channel. *Biophysical Journal*, Vol. 71, pg. 3064-3072.

Smith G.D., Wagner J., & Keizer J. (1996). Validity of the Rapid Buffering Approximation near a point source of Calcium ions. *Biophysical Journal*, Vol. 70, pg. 2527-2539.

Sneyd *et al*. (2006). A Buffering SERCA Pump in Models of Calcium Dynamics. *Biophysical Journal*, Vol. 91, pg.151-163.

Tewari S. & Pardasani K.R. (2008). Finite Difference Model to Study the Effects of Na^{+} Influx on Cytosolic Ca^{2+} Diffusion. *International Journal of Biological and Medical Sciences*, Vol. 1, 4, pg. 205-210.

Wagner J. & Keizer J. (1994). Effects of Rapid Buffers on Ca^{2+} Diffusion and Ca^{2+} Oscillations, *Biophysical Journal*, Vol. 67, pg. 447-456.

Table 1. Value of biophysical parameters used

Symbol	Parameter	Value	Reference
P_{ca}	Calcium permeability	$5.4x10^{-6}$ metre/sec	In this paper
P_{Na}	Sodium permeability	$6.07x10^{-10}$ metre/sec	(Tewari S. et al, 2008, p. 205-210)
F	Faraday's constant	96487coulomb/moles	known fact
R	Real gas constant	8.314 J/K mole	known fact
T	Absolute temperature	310°K	in this paper
z_{Ca}	Calcium valence	2	known fact
z_{Na}	Sodium valence	1	known fact
V_m	Resting Membrane potential	-70 mV	(Fain G.L., 1999)
D_{Ca}	Diffusion coefficient	250 $\mu m^2/s$	(Tewari S. et al, 2008, p. 205-210)
$(D_{Ca})^{ER}$	Diffusion coefficient	250 $\mu m^2/s$	In this paper
D_m	Mobile buffer diffusion coefficient	75 $\mu m^2/s$	(Jafri S. et al, 1995, p.2139-2153)
$(D_m)^{ER}$	Mobile buffer diffusion coefficient in ER	75 $\mu m^2/s$	(Jafri S. et al, 1995, p.2139-2153)
K_m	Mobile buffer disassociation rate	2 µM	(Smith G.D. et al, 1996, p.2527-2539)
K_m^{ER}	Mobile buffer disassociation rate	2 µM	In this paper
K_s	Stationary buffer disassociation rate	10 µM	In this paper
K_s^{ER}	Stationary buffer disassociation rate	10 µM	(Jafri S. et al, 1995, p.2139-2153)
K_{msod}	Sodium mobile buffer disassociation rate	10 mM	(Shannon T.R. et al, 2004, p. 3351-3371)
B_m	Mobile buffer concentration	75 µM	(Jafri S. et al, 1995, p.2139-2153)
B_m^{ER}	Mobile buffer concentration	250 µM	(Jafri S. et al, 1995, p.2139-2153)
B_s	stationary buffer concentration	225 µM	(Jafri S. et al, 1995, p.2139-2153)
B_s^{ER}	stationary buffer concentration	1 mM	In this paper
B_{msod}	Sodium mobile buffer concentration	5.35 mM	(Shannon T.R. et al, 2004, p. 3351-3371)
Ca_{out}	Extracellular calcium concentration	1.8 mM	(Shannon T.R. et al, 2004, p. 3351-3371)
Na_{out}	Extracellular sodium concentration	145 mM	(Shannon T.R. et al, 2004, p. 3351-3371)
Ca_i	Cytosolic calcium concentration	0.1 µM	(Shannon T.R. et al, 2004, p. 3351-3371)
Na_i	Cytosolic sodium concentration	12 mM	(Shannon T.R. et al, 2004, p. 3351-3371)
V_{SLPump}	Maximum pump capacity of PMCA	0.9 µM/sec	In this paper
K_{SLPump}	Half maximal pump capacity	0.1 µM	(Jafri S. et al, 1995, p.2139-2153)
H	Hill's coefficient	1.6	(Shannon T.R. et al, 2004, p. 3351-3371)
leakcons	Leak constant from ER	2.0 sec^{-1}	(Jafri S. et al, 1995, p.2139-2153)
ipflux	Maximum IP_3 flux rate	300 sec^{-1}	(Jafri S. et al, 1995, p.2139-2153)
volrat	Ratio of ER to cytoplasmic volume	0.185	(Jafri S. et al, 1995, p.2139-2153)
irbc	Inhibitory receptor binding constant	0.2 $\mu M^{-1}sec^{-1}$	(Jafri S. et al, 1995, p.2139-2153)
arbc	Activation receptor binding constant	20 $\mu M^{-1}sec^{-1}$	(Jafri S. et al, 1995, p.2139-2153)
irdc	Inhibitory receptor dissociation constant	0.2 sec^{-1}	(Jafri S. et al, 1995, p.2139-2153)
ardc	Activation receptor dissociation constant	$20x82.3x10^{-3}$ sec^{-1}	(Jafri S. et al, 1995, p.2139-2153)
scapumprate	SERCA maximal pump rate	45 µM/sec	(Jafri S. et al, 1995, p.2139-2153)
scadissrat	SERCA disassociation constant	0.1 µM	(Jafri S. et al, 1995, p.2139-2153)
Kcain	Calcium dependent inactivation	10 µM	(Kusters et al, 2005, p. 3741-3756)
ipin	External IP_3 input rate	2 µM/sec	(Keizer J. et al, 1992, p. 649-660)
ft	IP_3 pulse	1	In this paper
v_6	Maximum Ca^{2+} dependent IP_3 input rate	0.710 µM/sec	(Keizer J. et al, 1992, p. 649-660)
v_7	IP_3 decay rate constant	2.0 s^{-1}	(Keizer J. et al, 1992, p. 649-660)
k_6	Activation const.Ca^{2+} dependent IP_3 input	1.1 µM	(Keizer J. et al, 1992, p. 649-660)

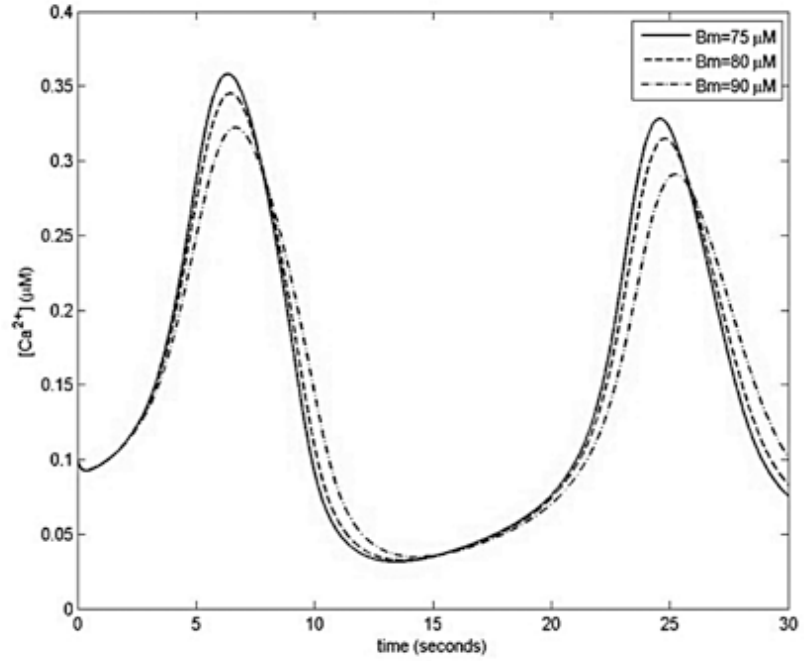

Figure 1. Variation of calcium with time and cytoplasmic buffer concentration

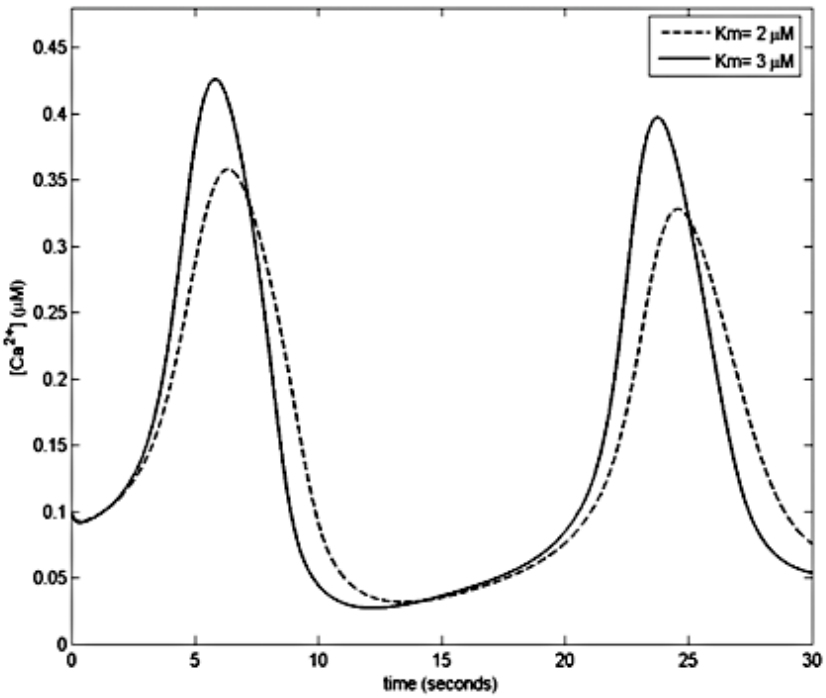

Figure 2. Variation of calcium with time and buffer dissociation rate

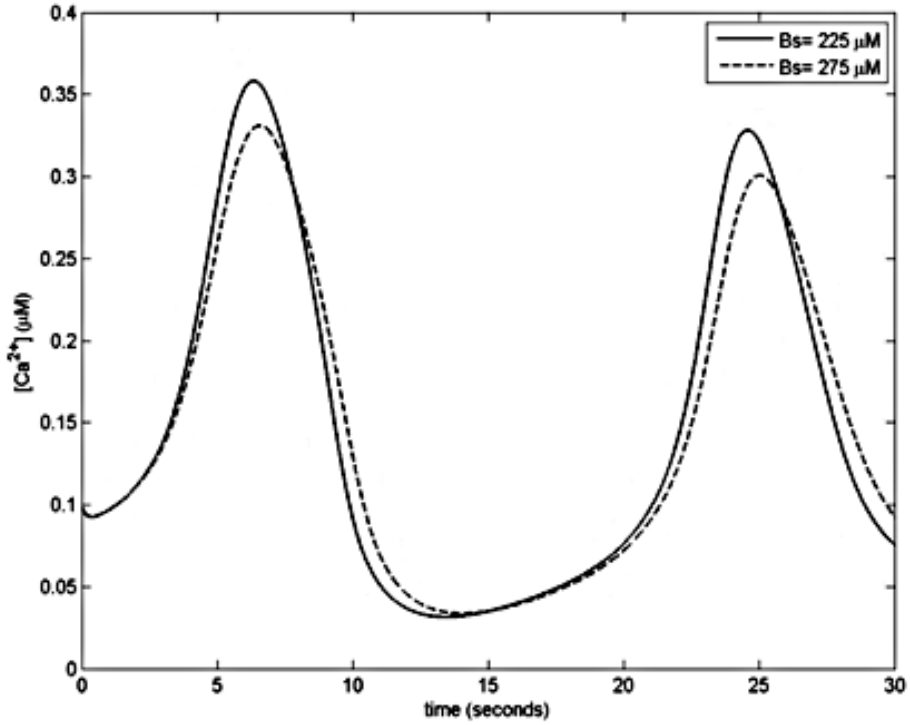

Figure 3. Calcium oscillation with time and stationary buffer concentration

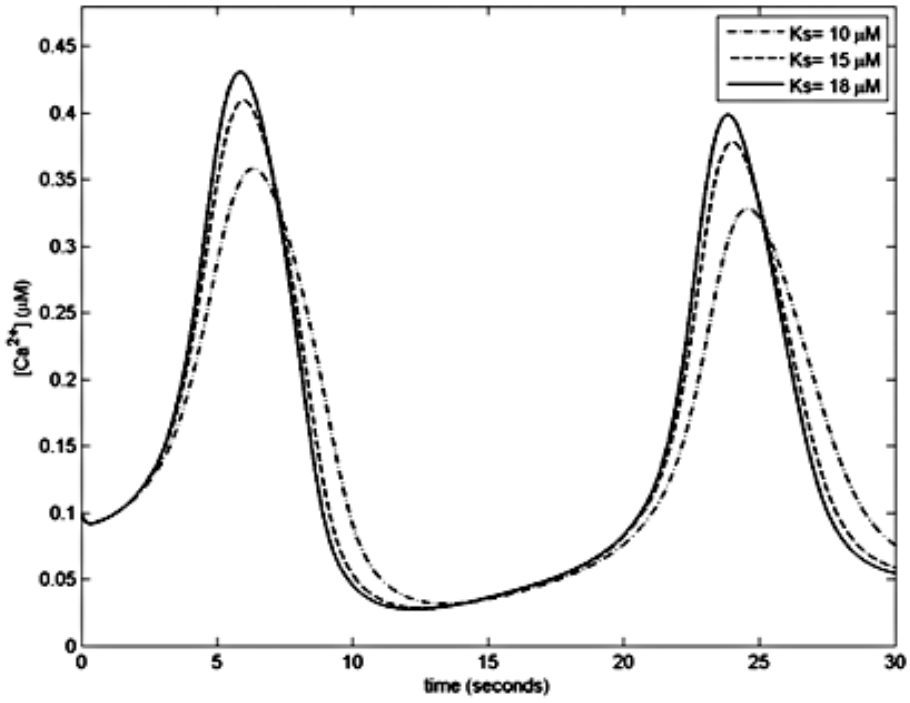

Figure 4. Calcium variation with time and stationary buffer disassociation rate

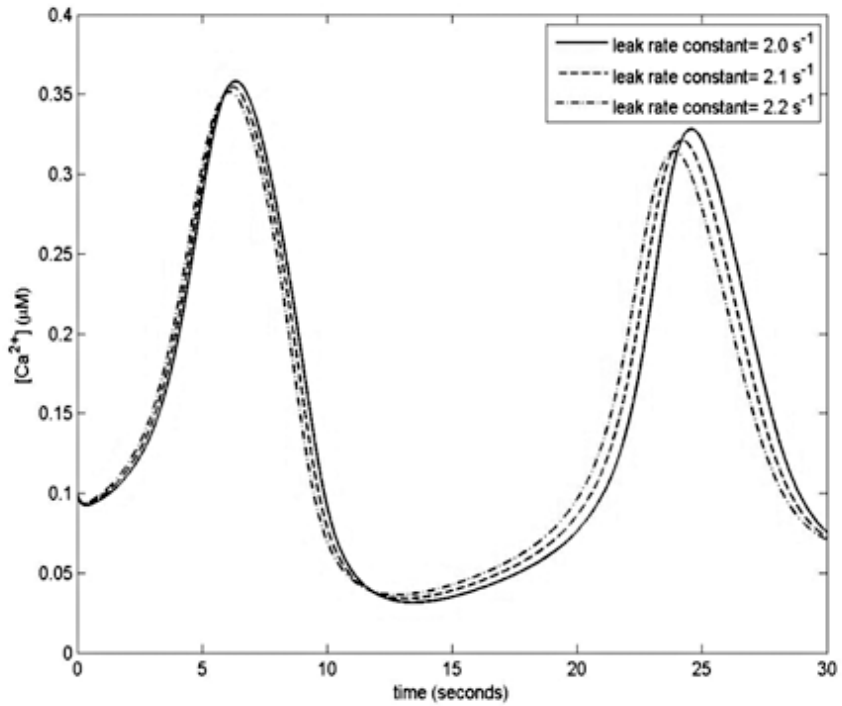

Figure 5. Calcium variation with leak rate constant

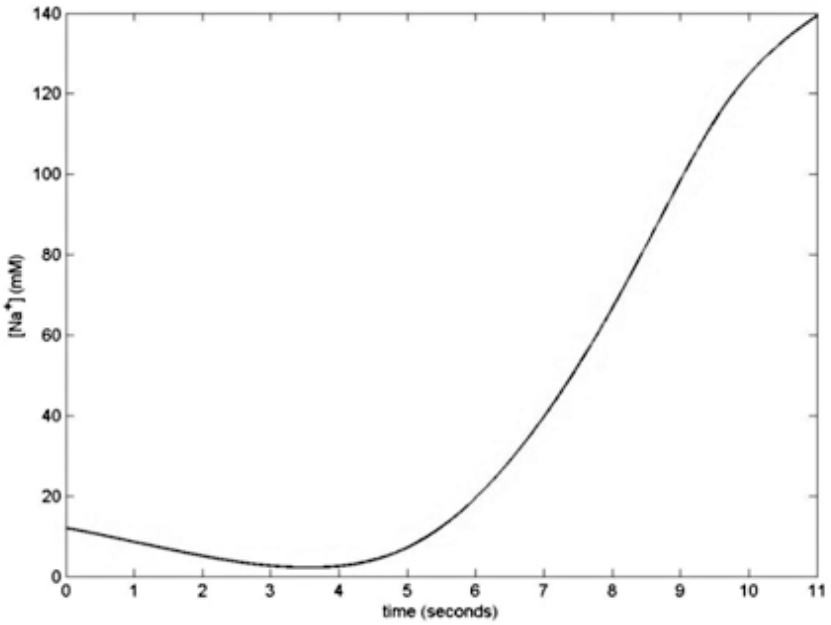

Figure 6. Sodium concentration variations with time

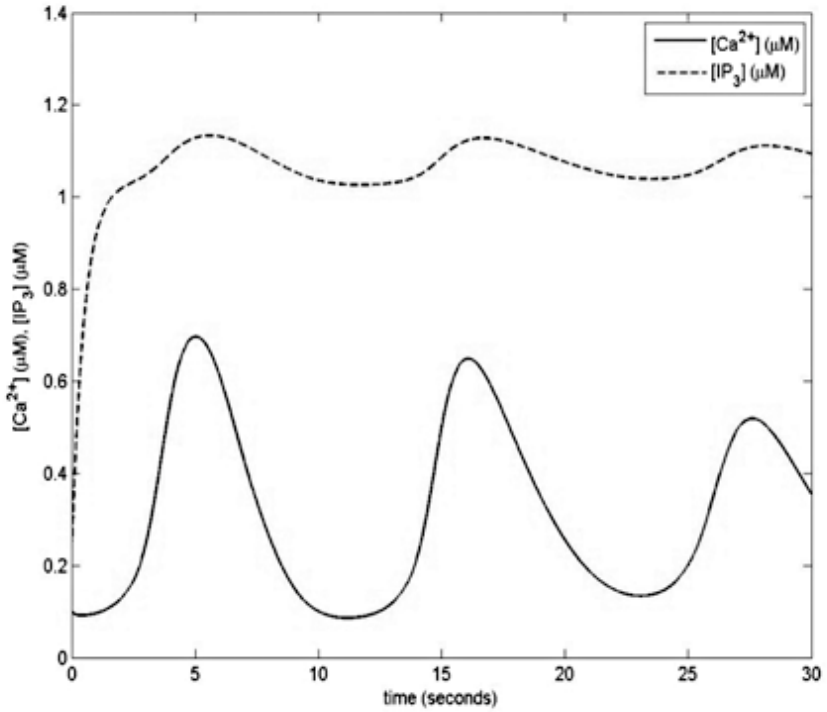

Figure 7. Variations in calcium and inositol triphosphate with time

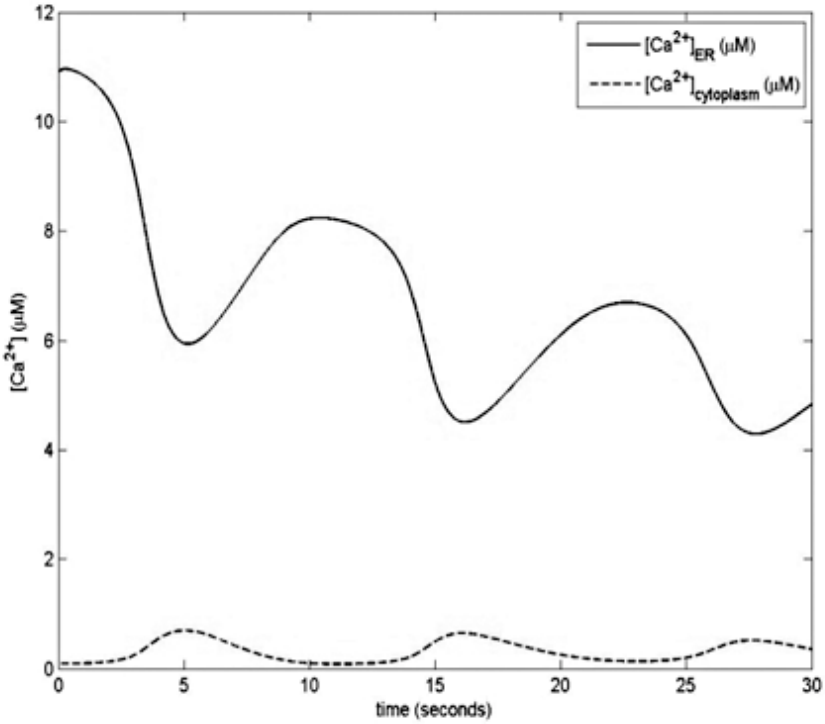

Figure 8. Variations in cytoplasmic and er calcium with time

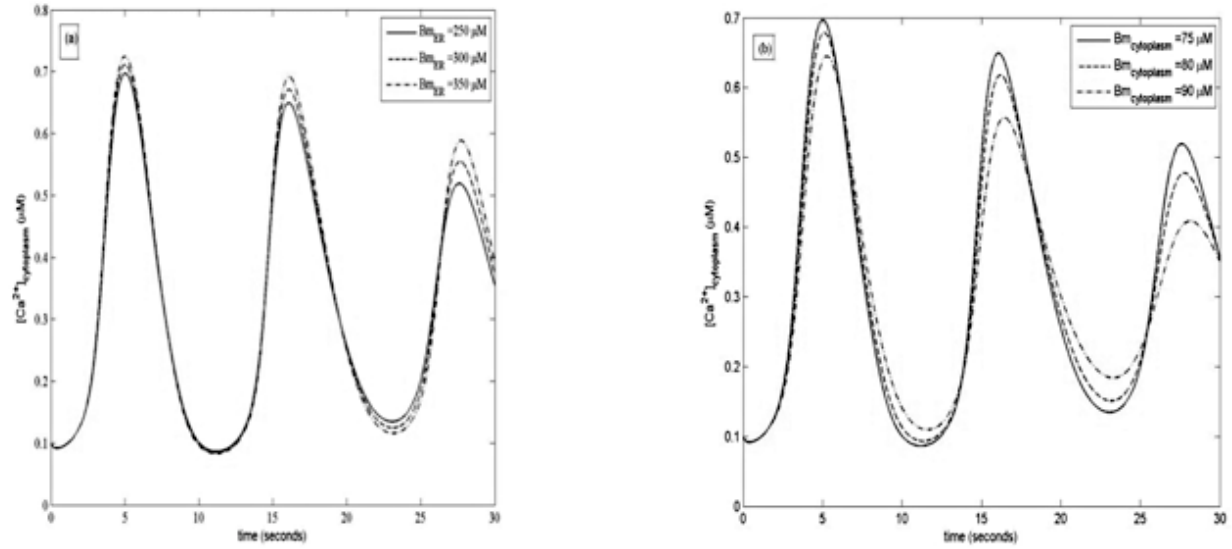

Figure 9. Variation of cytosolic calcium with time and (a) er and (b) cytoplasmic buffer concentrations

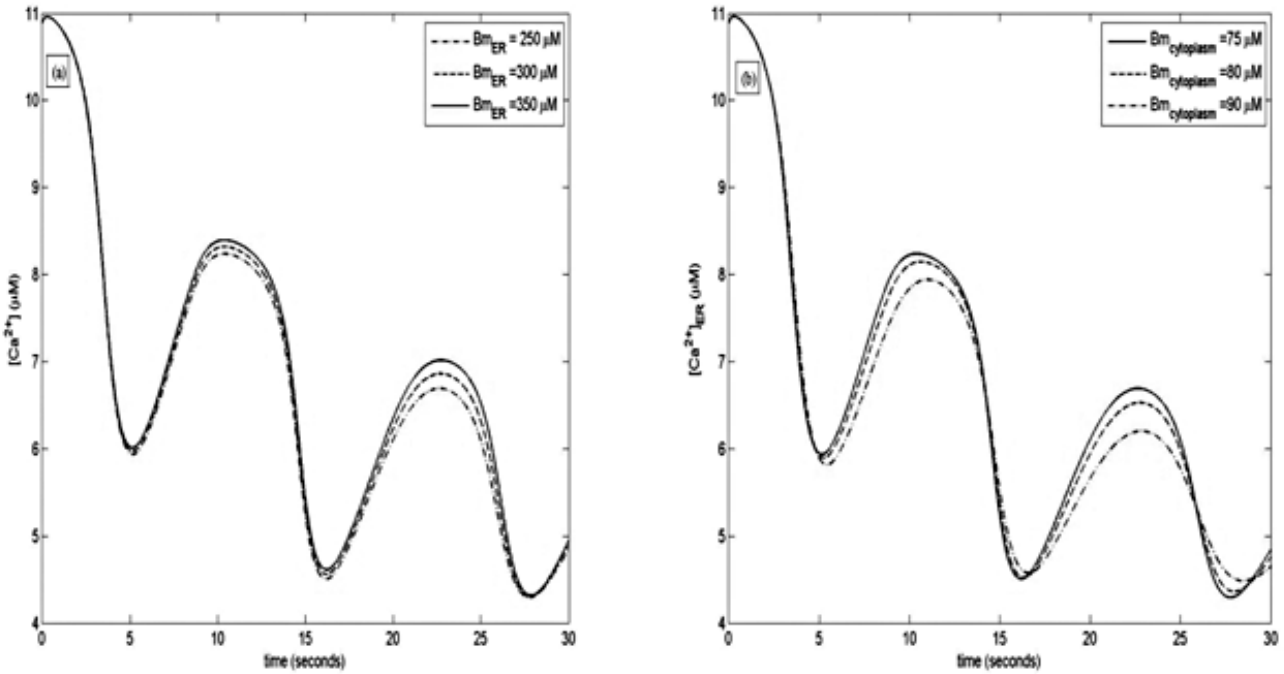

Figure 10. Plot of er calcium variation with (a) er and (b) cytoplasmic buffer concentration and time

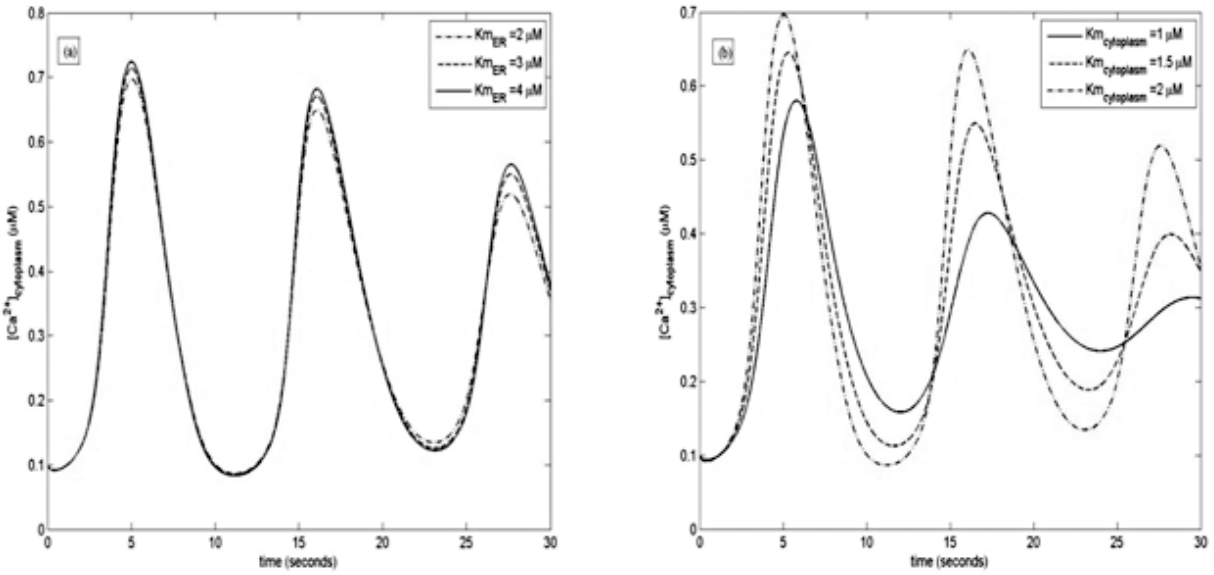

Figure 11. Cytosolic calcium variation with (a) er and (b) cytoplasmic buffer disassociation rate and time

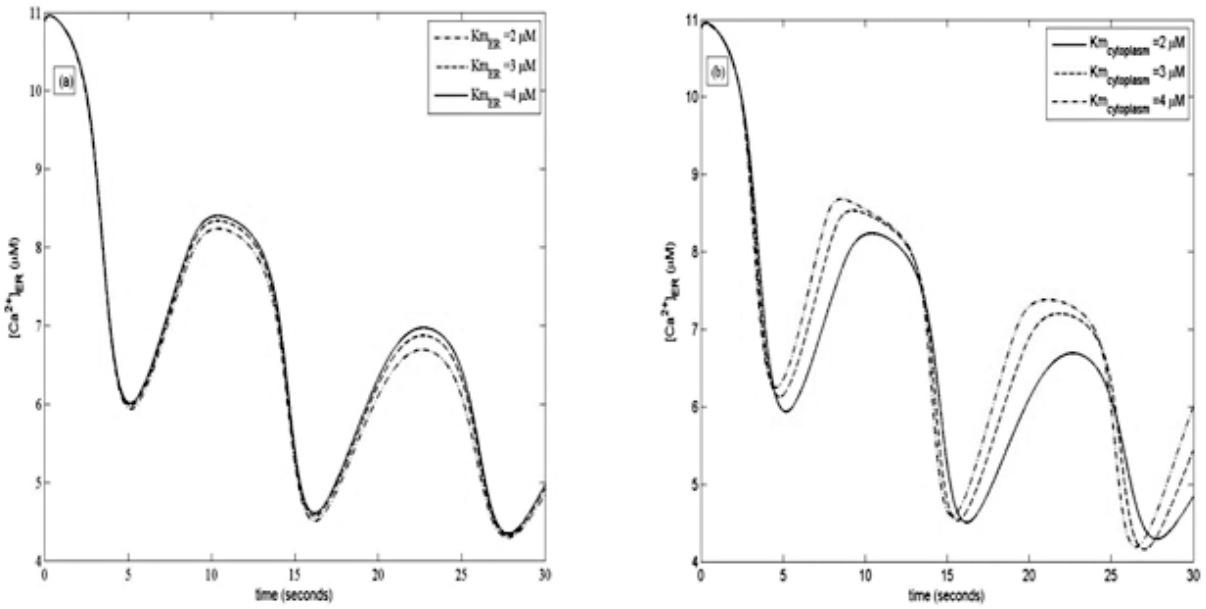

Figure 12. Plot of er calcium variation with (a) er and (b) cytoplasmic buffer disassociation rate and time